

An Explicit Spectral Collocation Method for the Drug Release Coronary Stents

Somayeh Fakhri and Sayed Hodjatollah Momeni-Masuleh

Department of Mathematics, Shahed University

Tehran, P. O. Box: 18151-159, Iran

E-mail(*corresp.*): momeni@shahed.ac.ir

E-mail: s.fakhri@shahed.ac.ir

Received June 7, 2021; revised May 25, 2022; accepted May 26, 2022

Abstract. This research aims to solve a comprehensive one-dimensional model of drug release from cardiovascular stents in which the drug binding is saturable and reversible. We used the Lagrange collocation method for space dimension and the modified Euler method for time discretization. The existence and uniqueness of the solution, are provided. The consistency, stability, and convergence analysis of the proposed scheme are provided, to show that numerical simulations are valid. Numerical results accurate enough and efficient just by using fewer mesh.

Keywords: spectral collocation method, explicit method, modified Euler method, stent, drug release.

AMS Subject Classification: 65M70; 65M20; 35K20; 35K57; 35Q92.

1 Introduction

Nowadays, one of the common causes of death is cardiovascular disease. The most common of them is a case of atherosclerosis which, occurs due to the accumulation of fat in the arterial wall. The early stages of the disease begin with an abnormal accumulation of cells and macrophages containing low-density lipoprotein (LDL) in the artery wall. The atherosclerotic plaque will be formed as the disease progress and macrophages increase. This plaque has a variable thickness as well as a core that consists of macrophages, smooth muscle cells, and lipids. As the disease progresses, the plaque grows and leads to narrowing of the lumen and occlusion of the arteries. It reduces blood flow and, in turn, reduces the level set of oxygen in the heart muscle and may lead

to a heart attack (due to death of the heart muscle) or stroke (due to tearing or blockage of blood vessels to the brain).

In the late 1980s and early 1990s, Palms introduced stenting as angioplasty to the medical community [12]. Stents with various designs and structures have widely used. Stenting has many advantages, including low-invasive and local anesthetic. Also, the rest and recovery time are significantly reduced compared with other methods. Several factors, including the size of the lesion, make it possible to use different stents, consisting of a metal structure, a polymer, and a drug-loaded in the polymer.

The first mathematical study was done on drug release stents by Zunino [19]. He considered just the layer of coating stent and the arterial wall as porous media and ignored the cellular layer, intima, and elastic laminate inside. He analyzed the dynamic of drug release from drug-eluting stents and focused on the influence of affective factors in drug-release, such as drug type, polymer coating, and its characteristics. Zunino et al. [20] outlined a complete overview of mathematical models and numerical methods used for drug stents and their interaction with the arterial wall. They provided a thorough study of mechanics, fluid dynamics, and drug release from cardiovascular stents through a mass transfer model coupled with a fluid dynamic model and used the finite element method to solve it. D'Angelo et al. [4] presented a drug release model for a drug-eluting stent and solved it using the finite element method in space and finite difference method in time. Ferreira et al. [6] proposed a 2D model for drug release from cardiovascular stents and obtained numerical results by using the implicit-explicit finite element method for spatial discretization and the Euler method for temporal discretization. Ferreira et al. [5] presented a 3D model for absorbing and releasing drugs in cylindrical matrices coated with a drug-loaded polymer. Their model contained a system of partial differential equations with boundary conditions and moving boundary. They proposed a coupled implicit-explicit method to solve the initial-boundary value problem. McGinty and Pontrelli [14] provided a comprehensive model for drug release from drug delivery devices in biological tissues. Their model included material release, solubility in polymeric coatings along with diffusion, convection, and biological tissue reaction as well as nonlinear saturation. They used a finite difference method to solve their model.

In this paper, the one-dimensional McGinty and Pontrelli [14] is solved using the lagrange collocation method in spatial discretization and the modified Euler method in time. We intend to use a lagrange collocation method based on derivative of Chebyshev polynomials using fewer mesh size to solve the problem in the desired domain at specified times, as well as, the consistency, stability, and convergence analysis of the proposed scheme. The numerical simulation exhibits the proficiency of the method.

2 Modeling description

This section concerns a comprehensive one-dimensional McGinty and Pontrelli model of drug release of cardiovascular stents that expressing absorption and diffusion of the drug in the polymeric coating stent and arterial wall. In this

model, there are two situations to deal with the drug: Dissolved drug and bounded drug. Many researchers (see, for example, [8]) believe that two main phenomena can occur in the release of solvent into the polymeric coating: The rate of solvent diffusion and the change in the internal structure of the polymer. Now, we describe the modeling of drug release in the polymer coating of the stent and the arterial wall.

2.1 Modeling of drug release in the polymeric matrix

A cardiovascular stent is a metallic scaffold covering a polymeric coating that contains a loaded drug. It is poached into a narrowed vessel to expand it. The stenting process is shown diagrammatically in Figure 1, and Figure 2 demonstrates the physical domain of the problem.

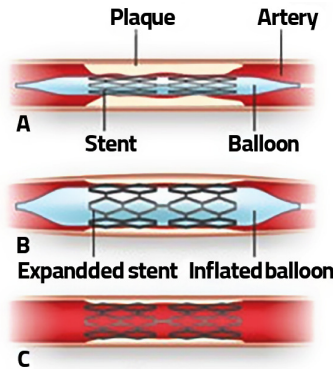


Figure 1. A schematic representation of the stenting process inside the blocked vessel [10].

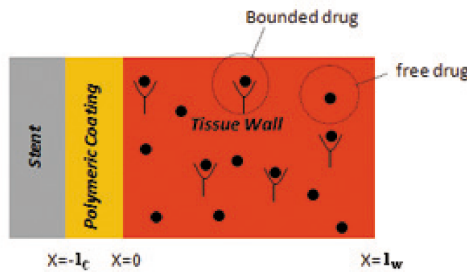


Figure 2. The geometric configuration of the stent consists of a metallic structure (gray) coated with a layer of polymeric of thickness l_c (orange) containing the drug (black). The polymeric coating is in contact with the biological tissue of thickness l_w (red).

The loaded-drug in the cardiovascular stent requires to dissolve to release and absorb in the arterial wall. By exposing the polymeric coating in the vicinity of the biofluid, it becomes wetted, and a dissolution process begins. The circumstances for drug release is ready now. It is often desirable that

the drug is hydrophobic because of its poor ability to dissolve and helps to protect the drug in the arterial wall. The dissolution process depends not only on the solubility but also on the degree of solubility of the drug in the biofluid. Considering these two factors, it has an essential effect on the drug release rate. Multiple approaches have been proposed to model the dissolution process in which usually the initial concentration of the loaded drug in the polymer coating, B_0 , is considered more than its solvability, S ; otherwise, the drug easily is dissolved and diffused. Thus it rarely is divided into two distinct phases. Here, the encapsulated drug considered a continuous variable, and it assumed that the biofluid enters into the porous polymeric coating immediately and becomes wetted it. The dissolution and the release of loaded drug in the polymeric coating are described by a system of partial differential equations as follows [14]

$$\frac{\partial b_c(t, x)}{\partial t} = -\beta_c b_c^\alpha(t, x) (S - c_c(t, x)) \quad \text{in } (-l_c, 0), \quad (2.1)$$

$$\frac{\partial c_c(t, x)}{\partial t} = D_c \frac{\partial^2 c_c(t, x)}{\partial x^2} + \beta_c b_c^\alpha(t, x) (S - c_c(t, x)) \quad \text{in } (-l_c, 0), \quad (2.2)$$

where $c_c(t, x)$ and $b_c(t, x)$ are the concentrations of the dissolved and undissolved drug in the polymeric coating, respectively; D_c is the effective diffusion coefficient of the drug; β_c is the dissolution rate which its unit, i.e., $\left(\frac{1}{s \cdot (\text{mol} \cdot \text{cm}^{-3})^\alpha}\right)$ is dependent on the value of α [14]. The amount of α depends on the geometric composition, chemical properties, coating structure, and stent design. In the Noyes-Whitney approach, the dissolution rate is considered proportional to the difference between drug dissolution and dissolved drug concentration, which led to the linear equation ($\alpha = 0$) [15]. Hixson and Crowell [9] made corrections that attempted to account for the variation in the level of dissolved particles, which led to a nonlinear model of the dissolution ($\alpha = \frac{2}{3}$) [14]. The case $\alpha = 1$, deals with the simplest nonlinear dissolution model that couples two distinct phases, i.e., free and bonded phases. The case $\alpha = \frac{2}{3}$, represented by [7]. Model (2.1)–(2.2) is an integrated model of previous models and is valid when the dissolution is in progress. When the solid drug was solved ($b_c = 0$), the source sentence in the model becomes zero.

2.2 Drug binding formulation

There are different binding formulations which may be linear or nonlinear, saturated or unsaturated, and reversible or irreversible, depending on the type of dissolved drug and cardiovascular stent. The concentration of the binding drug in the arterial wall, i.e., $b_w(t, x)$ is given by [14]

$$\frac{\partial b_w(t, x)}{\partial t} = k_f c_w(t, x) (b_{max} - b_w(t, x)) - k_b b_w(t, x) \quad \text{in } (0, l_w), \quad (2.3)$$

where $c_w(t, x)$ is the concentration of the dissolved drug in the arterial wall; k_f is the forward rate constant; k_b is the backward rate constant; b_{max} is the local density of binding sites.

2.3 Drug transport formulation

The equation for the transfer of the dissolved drug in the arterial wall is given by

$$\frac{\partial c_w(t, x)}{\partial t} = D_w \frac{\partial^2 c_w}{\partial x^2} - \nu \frac{\partial c_w(t, x)}{\partial x} - k_f c_w(t, x)(b_{max} - b_w(t, x)) - k_b b_w(t, x) \quad \text{in } (0, l_w), \quad (2.4)$$

where D_w denotes the diffusion coefficients of the dissolved drug in the wall and ν is a convective velocity positive constant.

3 A comprehensive 1D coupled model of drug release

When the diffusion-dissolution formulation of the polymeric coating of the cardiovascular stent, (2.1)–(2.2), is coupled with the nonlinear binding formulation and the diffusion-convection formulation in the arterial wall, (2.3)–(2.4), we arrive at a comprehensive coupled model of the drug release in the cardiovascular stent. The model requires some information about the boundary, initial, and interface conditions.

3.1 Boundary, initial, and interface conditions

The Robin boundary conditions at $x = -l_c$ and $x = l_w$ are as follows

$$\begin{aligned} -D_c \frac{\partial c_c(t, x)}{\partial x} &= 0 & \text{at } x = -l_c, \\ -D_w \frac{\partial c_w(t, x)}{\partial x} + \nu c_w(t, x) &= \lambda_w c_w(t, x) & \text{at } x = l_w, \end{aligned}$$

where λ_c and λ_w are the constants to coincides with the observed conditions experimentally.

The initial conditions are

$$b_c(x, 0) = B_0, \quad c_c(x, 0) = 0, \quad c_w(x, 0) = 0, \quad b_w(x, 0) = 0.$$

As the continuity condition exists in the interface between the polymeric coating and the arterial wall, the interface condition may consider as

$$-D_c \frac{\partial c_c(t, x)}{\partial x} = -D_w \frac{\partial c_w(t, x)}{\partial x} + \nu c_w(t, x) \quad \text{at } x = 0.$$

Also, there may be a jump on the concentration in the interface, i.e.,

$$-D_w \frac{\partial c_w(t, x)}{\partial x} = P(c_c(t, x) - c_w(t, x)) \quad \text{at } x = 0,$$

where $P(cm/s)$ is the total mass transfer coefficient. Here, although the equations are interdependent, we do not combine them, instead, we treat each domain independently and use the first domain data to obtain the values of variables in the second domain.

3.2 Non-dimensionalized drug release model

In the derivation of the new non-dimensionalized equations, the set of variables of time and space transformed into a new set of variables $\tilde{x} = x/l_w$, $\tilde{t} = D_w t/l_w^2$. Here, the parameters of the arterial wall used as the reference data. All concentrations scaled in the initial amount of B_0

$$\begin{aligned} \tilde{b}_c(t, x) &= \frac{b_c(t, x)}{B_0}, & \tilde{c}_c(t, x) &= \frac{c_c(t, x)}{B_0}, \\ \tilde{b}_w(t, x) &= \frac{b_w(t, x)}{B_0}, & \tilde{c}_w(t, x) &= \frac{c_w(t, x)}{B_0}, & \tilde{b}_{max} &= \frac{b_{max}}{B_0}. \end{aligned}$$

By setting the following parameters:

$$\begin{aligned} D &= \frac{D_c}{D_w}, & L &= \frac{l_c}{l_w}, & D_\alpha &= \frac{\beta_c B_0^{\alpha-1} S l_w^2}{D_w}, & \Lambda_c &= \frac{\lambda_c l_w}{D_w}, & \Theta &= \frac{P l_w}{D_w}, \\ D_w^* &= \frac{k_f l_w^2 b_{max}}{D_w}, & \beta_p &= \frac{l_w^2}{k_b D_w}, & \Lambda_w &= \frac{\lambda_w l_w}{D_w}, & P \acute{e} &= \frac{\nu l_w}{D_w}, \end{aligned}$$

and employing them into Equation (2.1) leads to

$$\frac{\partial b_c(t, x)}{\partial t} = -D_\alpha B_0 b_c^\alpha S \left(1 - \frac{c_c(t, x)}{S}\right) \quad \text{in } (-L, 0). \tag{3.1}$$

In a similar fashion and using some manipulation on Equations (2.2), (2.3), and (2.4), the resulting equations read as follows

$$\frac{\partial c_c(t, x)}{\partial t} = D \frac{\partial^2 c_c(t, x)}{\partial x^2} + D_\alpha B_0 b_c^\alpha S \left(1 - \frac{c_c(t, x)}{S}\right) \quad \text{in } (-L, 0), \tag{3.2}$$

$$\frac{\partial b_w(t, x)}{\partial t} = D_w^* B_0 \left[c_w(t, x) \left(1 - \frac{b_w(t, x)}{b_{max}}\right) \right] - \frac{b_w(t, x)}{\beta_p} \quad \text{in } (0, 1),$$

$$\begin{aligned} \frac{\partial c_w(t, x)}{\partial t} &= \frac{\partial^2 c_w(t, x)}{\partial x^2} - P \acute{e} \frac{\partial c_w(t, x)}{\partial x} \\ &\quad - D_w^* B \left[c_w(t, x) \left(1 - \frac{b_w(t, x)}{b_{max}}\right) \right] + \frac{b_w(t, x)}{\beta_p} \quad \text{in } (0, 1). \end{aligned} \tag{3.3}$$

In the same way as before, non-dimensionalized boundary and interface conditions are derived as

$$\begin{aligned} D \frac{\partial c_c(t, x)}{\partial x} &= 0 && \text{at } x = -L, \\ \frac{\partial c_w(t, x)}{\partial x} &= \Theta (c_c(t, x) - c_w(t, x)) && \text{at } x = 0, \\ -D \frac{\partial c_c(t, x)}{\partial x} &= -\frac{\partial c_w(t, x)}{\partial x} + P \acute{e} c_w(t, x) && \text{at } x = 0, \\ -\frac{\partial c_w(t, x)}{\partial x} + P \acute{e} c_w(t, x) &= \Lambda_w c_w(t, x) && \text{at } x = 1. \end{aligned}$$

4 Explicit Lagrange collocation scheme

This section presents the details of the scheme, which contains the Lagrange collocation and the modified Euler method that is used for the spatial and temporal discretization, respectively.

4.1 Spatial discretization

The Lagrange collocation method uses a strong formulation of the equation. In this method, the approximate solution is required to satisfy the differential equation at a set of discrete points exactly, which called collocation points. The nodal bases, Lagrange polynomials used to implement the Lagrange collocation method. Suppose $\Omega \subset \mathbb{R}$, which divided into N disjoint sub-intervals. The Gauss-Lobatto points assumed as collocation points. The nodes and weights of the Gauss-Lobatto quadrature formula relative to the Chebyshev weight $w(x) = \sqrt{1 - x^2}$ is given by [3]

$$\begin{aligned} w_0 = w_N &= \frac{\pi}{2N}, \quad w_k = \frac{\pi}{N}, \quad k = 1, 2, \dots, N - 1, \\ x_j &= \cos\left(\frac{\pi j}{N}\right), \quad j = 0, 1, \dots, N. \end{aligned} \tag{4.1}$$

For these nodes, (4.1), Lagrange polynomials ψ_l of degree N can be expressed as [3]

$$\psi_l(x) = \frac{(-1)^{(l+1)}(1 - x^2)T'_N(x)}{\bar{c}_l N^2(x - x_l)}, \quad l = 0, 1, \dots, N, \tag{4.2}$$

where $T'_N(x)$ is a derivative of Chebyshev polynomial, and \bar{c}_l is

$$\bar{c}_l = \begin{cases} 2, & l = 0, N, \\ 1, & l = 1, \dots, N - 1. \end{cases}$$

By using the Chebyshev polynomial, each sub-interval of the physical domain Ω must convert to $[-1, 1]$. Now, we approximate the concentration functions using the following expansions:

$$c_j^N(t, x) = \sum_{i=0}^N c_{j_i}(t)\psi_i(x), \quad j = c, w, \tag{4.3}$$

$$b_j^N(t, x) = \sum_{i=0}^N b_{j_i}(t)\psi_i(x), \quad j = c, w, \tag{4.4}$$

where

$$\psi_i(x_k) = \delta_{i,k}. \tag{4.5}$$

The first and second derivatives of $c_j^N(t, x)$ are

$$\frac{\partial c_j^N(t, x)}{\partial x} = \sum_{i=0}^N c_i(t)\psi'_i(x), \quad \frac{\partial^2 c_j^N(t, x)}{\partial x^2} = \sum_{i=0}^N c_i(t)\psi''_i(x). \tag{4.6}$$

The closed forms for the first-derivative and second derivative matrices, respectively, are [3]

$$\begin{aligned}
 (\mathbf{D}_N)_{jl} &= \begin{cases} \frac{\bar{c}_j}{\bar{c}_l} \frac{(-1)^{j+l}}{x_j - x_l}, & j \neq l, \\ -x_j/2(1 - x_l^2), & 1 \leq j = l \leq N - 1, \\ (2N^2 + 1)/6, & j = l = 0, \\ -(2N^2 + 1)/6, & j = l = N, \end{cases} \tag{4.7} \\
 (\mathbf{D}_N^2)_{jl} &= \begin{cases} \frac{(-1)^{j+l}}{\bar{c}_l} \frac{x_j^2 + x_j x_l - 2}{(1 - x_j^2)(x_j - x_l)^2} 1 \leq j \leq N - 1, & 0 \leq l \leq N, \quad j \neq l, \\ -\frac{(N^2 - 1)(1 - x_j^2) + 3}{3(1 - x_j^2)^2}, & 1 \leq j = l \leq N - 1, \\ \frac{2}{3} \frac{(-1)^l}{\bar{c}_l} \frac{(2N^2 + 1)(1 - x_l) - 6}{(1 - x_l^2)}, & j = 0, \quad 1 \leq l \leq N, \\ \frac{2}{3} \frac{(-1)^{l+N}}{\bar{c}_l} \frac{(2N^2 + 1)(1 + x_l) - 6}{(1 + x_l^2)}, & j = N, \quad 0 \leq l \leq N, \\ (N^4 - 1)/15, & j = l = 0, \quad j = l = N. \end{cases}
 \end{aligned}$$

At $\xi_0 = -1$ ($x = -L$) by inserting (4.3), (4.4) and (4.6) into (3.1)–(3.2) and utilizing (4.5), we have the following system of equations:

$$\begin{aligned}
 \frac{\partial b_c^N}{\partial t}(t, \xi_0) &= -D_\alpha B_0 (b_{c_0}(t))^\alpha S \left(1 - \frac{c_{c_0}(t)}{S} \right), \\
 \frac{\partial c_c^N}{\partial t}(t, \xi_0) &= D_\alpha B_0 (b_{c_0}(t))^\alpha S \left(1 - \frac{c_{c_0}(t)}{S} \right).
 \end{aligned}$$

For $\xi_k \in (-1, 1)$ ($x \in (-L, 0)$), $k = 1, \dots, N - 1$, doing a similar process, we get

$$\begin{aligned}
 \frac{\partial b_c^N}{\partial t}(t, \xi_k) &= -D_\alpha B_0 (b_{c_k}(t))^\alpha S \left(1 - \frac{c_{c_k}(t)}{S} \right), \\
 \frac{\partial c_c^N}{\partial t}(t, \xi_k) &= D \sum_{i=0}^N c_{c_i}(t) \psi_i''(\xi_k) + D_\alpha B_0 (b_{c_k}(t))^\alpha S \left(1 - \frac{c_{c_k}(t)}{S} \right).
 \end{aligned}$$

At $\xi_N = 1$ ($x = 0$), which is the interface boundary, we can write

$$\begin{aligned}
 \frac{\partial b_c^N}{\partial t}(t, \xi_N) &= -D_\alpha B_0 (b_{c_N}(t))^\alpha S \left(1 - \frac{c_{c_N}(t)}{S} \right), \tag{4.8} \\
 \frac{\partial c_c^N}{\partial t}(t, \xi_N) &= c_{w_N}(t) \psi_N''(\xi_N) + P \acute{e} c_{w_N}(t) \psi_N'(\xi_N) \\
 &\quad + D_\alpha B_0 (b_{w_N}(t))^\alpha S \left(1 - \frac{c_{w_N}(t)}{S} \right).
 \end{aligned}$$

The above collocation equations give rise to the following system of ordinary differential equations:

$$\frac{d\tilde{\mathbf{u}}_c^N}{dt} + \mathbf{A}_{1_e} \tilde{\mathbf{u}}_c^N = \mathbf{f}(\tilde{\mathbf{u}}_c^N), \tag{4.9}$$

where $\tilde{\mathbf{u}}_c^N = (b_c^N(t), c_c^N(t))^T$. At the beginning of the arterial wall, i.e., at $\xi_0 = 1$ ($x = 0$), we have

$$\begin{aligned} \frac{\partial b_w^N}{\partial t}(t, \xi_0) &= D_w^* B_0 \left[c_{w_0}(t) \left(1 - \frac{b_{w_0}(t)}{b_{max}} \right) \right] - \frac{b_{w_0}(t)}{\beta_p}, \\ \frac{\partial c_w^N}{\partial t}(t, 0) &= \Theta \left(c_{w_0}(t) \psi'_0(\xi_0) - c_{c_0}(t) \psi'_0(\xi_0) \right) - \Theta (c_{w_0}(t) - c_{c_0}(t)) \\ &\quad - P\acute{e} c_{w_0}(t) \psi'_0(\xi_0) - D_w^* B \left[c_{w_0}(t) \left(1 - \frac{b_{w_0}(t)}{b_{max}} \right) \right] + \frac{b_{w_0}(t)}{\beta_p}. \end{aligned}$$

For $x \in (0, 1)$, we obtain the following system of equations:

$$\begin{aligned} \frac{\partial b_w^N}{\partial t}(t, \xi_k) &= D_w^* B_0 \left[c_{w_k}(t) \left(1 - \frac{b_{w_k}(t)}{b_{max}} \right) \right] - \frac{b_{w_k}(t)}{\beta_p}, \\ \frac{\partial c_w^N}{\partial t}(t, \xi_k) &= \sum_{i=0}^N c_{w_i}(t) \psi''_i(\xi_k) - P\acute{e} \sum_{i=0}^N c_{w_i}(t) \psi'_i(\xi_k) \\ &\quad - D_w^* B \left[c_{w_k}(t) \left(1 - \frac{b_{w_k}(t)}{b_{max}} \right) \right] + \frac{b_{w_k}(t)}{\beta_p}, \quad k = 1, \dots, N - 1. \end{aligned}$$

Finally, for $\xi_N = -1$ ($x = 1$), we have

$$\begin{aligned} \frac{\partial b_w^N}{\partial t}(t, \xi_N) &= D_w^* B_0 \left[c_{w_N}(t) \left(1 - \frac{b_{w_N}(t)}{b_{max}} \right) \right] - \frac{b_{w_N}(t)}{\beta_p}, \\ \frac{\partial c_w^N}{\partial t}(t, \xi_N) &= c_{w_N}(t) (\Lambda_w - P\acute{e}) \psi'_N(\xi_N) - P\acute{e} c_{w_N}(t) (\Lambda_w - P\acute{e}) \quad (4.10) \\ &\quad - D_w^* B \left[c_{w_N}(t) \left(1 - \frac{b_{w_N}(t)}{b_{max}} \right) \right] + \frac{b_{w_N}(t)}{\beta_p}. \end{aligned}$$

In the above equations, we use first and second derivative matrices to compute ψ' and ψ'' .

Collocation Equations (4.8)–(4.10) give rise to the following system of ordinary differential equations:

$$\frac{d\tilde{\mathbf{v}}_w^N}{dt} + \mathbf{A}_{2_w} \tilde{\mathbf{v}}_w^N = \mathbf{g}(\tilde{\mathbf{v}}_w^N), \quad (4.11)$$

where $\tilde{\mathbf{v}}_w^N = (b_w^N(t), c_w^N(t))^T$.

4.2 Time discretization

The systems of ODEs resulting from the spatial discretization, (4.9) and (4.11), have $4N + 4$ unknowns c_c^N , c_w^N , b_c^N , and b_w^N , which are solved independently using the modified Euler method over time. In this approach, the computed solution of the system (4.9), is used as the initial solution for solving the system (4.11) at any time.

5 Existence and uniqueness of the solution

In this section, we show the existence and uniqueness of the solution of Equation (4.9). We begin by proving the following theorem.

Theorem 1. *Suppose that $U \subseteq \mathbb{R}^n$ is an open region, $A : [-a, a] \rightarrow \mathbb{R}^{n \times n}$ is a continuous matrix-valued mapping, and $g : [-a, a] \times U \rightarrow U$ is a map of class C^1 . Then there exists $a > 0$ such that the following initial value problem has a unique solution for $t_0 \in [-a, a]$*

$$\begin{cases} \dot{x} = A(t)x + g(t, x), \\ x(t_0) = x_0. \end{cases} \tag{5.1}$$

Proof. We assume that $J = [-a, a]$, where a is dependent on the norm of the matrix A . By integrating the system (5.1) in time, we arrive at

$$x(t) = x(t_0) + \int_{t_0}^t A(s)x(s) + g(x, s) ds,$$

whose every solution is also a solution of the original system (5.1), and vice versa [1]. Let us $X = C^0(J, \mathbb{R}^{n \times n})$ with $a > 0$. We know that $\mathbb{R}^{n \times n}$ with sup-norm is a Banach space, so X is a Banach space concerning the following norm:

$$\|A\|_X = \sup\{\|A(t)\| : t \in J\}.$$

As we know, g is locally Lipschitz. By defining the mapping $T : X \rightarrow X$ as

$$Tx(t) = x(t_0) + \int_{t_0}^t A(s)x(s) + g(x, s) ds,$$

we see that

$$\begin{aligned} \|(Tx) - (Ty)\|_X &= \sup_{t \in J} \{ \|(Tx(t)) - (Ty(t))\| \} \\ &\leq \sup_{t \in J} \left\{ \left\| \int_{t_0}^t A(s)x(s) + g(x, s) ds - \int_{t_0}^t A(s)y(s) + g(y, s) ds \right\| \right\} \\ &\leq \sup_{t \in J} \int_{t_0}^t \|A(s)x(s) + g(x, s) - A(s)y(s) - g(y, s)\| ds \\ &\leq 2a\|A\|_X \|x - y\|_X + 2a\|g(x) - g(y)\|_X. \end{aligned}$$

Since g is Lipschitz, it follows that there exists a constant $M > 0$ such that

$$\|(Tx) - (Ty)\|_X \leq 2a\|A\|_X \|x - y\|_X + 2aM \|x - y\|_X.$$

Thus the contraction property of the mapping T can be obtained by choosing $a < \frac{1}{2(M+\|A\|_X)}$. As a result, T is a contraction mapping that maps A into itself. Therefore, according to the Banach fixed-point theorem [16], T has a unique fixed point in A , i.e., $T(x(t)) = x(t)$, so we have

$$x(t) = x(t_0) + \int_{t_0}^t A(s)x(s) + g(x, s) ds,$$

which is the solution of (5.1). The above argument implies the existence and uniqueness of the solution of (5.1).

As $\mathbf{f}(\mathbf{u}_c^N)$ is a Lipschitz function and \mathbf{A}_{1_c} is a continuous matrix-valued mapping, referring to Theorem 1, Equation (4.9) has a unique solution.

The same conclusion can be drawn for Equation (4.11).

6 Consistency, stability and convergence analysis

This section provides the consistency, stability, and convergence analysis of the scheme.

To check the consistency of the scheme, we assume that X_N is a subspace of \mathbb{P}_N , where \mathbb{P}_N is the polynomial of degree at most N . Let us define projection operator $I_N : \mathcal{W} \rightarrow X_N$, where is also an interpolation operator in which $\mathcal{W} \subseteq H^2(\Omega)$. Let c be the exact solution and c^N be the approximate solution. Then we have

$$\|c - c^N\|_{L^2_w} \leq \|c - I_N(c)\|_N + \|c^N - I_N(c)\|_N,$$

where $\|\cdot\|_N$ is the discrete norm. Using the equivalence of discrete and continuous norms, one can easily show that the right-hand side of the above equation tends to zero (see, for example, [3]).

To prove the stability, let us consider the discretized form of Equation (3.3) at (t, x_k) , for $k = 0, \dots, N$ as follows

$$\left(\frac{\partial c_w^N}{\partial t} - \frac{\partial^2 c_w^N}{\partial x^2} + P\acute{e} \frac{\partial c_w^N}{\partial x} \right) \Big|_{(t, x_k)} = D_w^* B \left[c_w^N \left(1 - \frac{b_w^N}{b_{max}} \right) - \frac{b_w^N}{\beta_p} \right] \Big|_{(t, x_k)}. \tag{6.1}$$

Multiplying the k^{th} equation of (6.1) by $c_w^N(t, x_k)w_k$ and summing over k , gives

$$\begin{aligned} & \frac{1}{2} \frac{d}{dt} \sum_{k=0}^N [c_w^N(t, x_k)]^2 w_k - \sum_{k=0}^N \frac{\partial^2 c_w^N}{\partial x^2}(t, x_k) c_w^N(t, x_k) w_k \\ & + P\acute{e} \sum_{k=0}^N \frac{\partial c_w^N}{\partial x}(t, x_k) c_w^N(t, x_k) w_k = \sum_{k=0}^N f(c_w^N) c_w^N(t, x_k) w_k, \end{aligned}$$

where

$$f(c_w^N(t, x_k)) = D_w^* B \left[c_w^N(t, x_k) \left(1 - \frac{b_w^N(t, x_k)}{b_{max}} \right) - \frac{b_w^N(t, x_k)}{B_p} \right].$$

As we know, for Gauss-Lobatto nodes (4.1) the Gaussian quadrature is exact for all polynomial of degree at most $2N + 1$. Since $\frac{\partial^2 c_w^N}{\partial x^2}(t, \cdot) c_w^N(t, \cdot)$ is a polynomial of degree $2N - 2$ and $\frac{\partial c_w^N}{\partial x}(t, \cdot) c_w^N(t, \cdot)$ is a polynomial of degree $2N - 1$, we may write

$$\begin{aligned} & \frac{1}{2} \frac{d}{dt} \sum_{k=0}^N [c_w^N(t, x_k)]^2 w_k - \int_{-1}^1 \frac{\partial^2 c_w^N}{\partial x^2}(t, x) c_w^N(t, x) w(x) dx \\ & + P\acute{e} \int_{-1}^1 \frac{\partial c_w^N}{\partial x}(t, x) c_w^N(t, x) w(x) dx = \sum_{k=0}^N f(c_w^N) c_w^N(t, x_k) w_k. \end{aligned} \tag{6.2}$$

Thanks to the following inequality (see Sect. 7.1.2 in [3])

$$-\int_{-1}^1 \frac{\partial^2 c_w^N}{\partial x^2}(t, x) c_w^N(t, x) w(x) dx \geq \frac{1}{4} \int_{-1}^1 \left[\frac{\partial c_w^N}{\partial x}(t, x) \right]^2 w(x) dx,$$

equation (6.2) becomes

$$\begin{aligned} & \frac{1}{2} \frac{d}{dt} \sum_{k=0}^N [c_w^N(t, x_k)]^2 w_k + \frac{1}{4} \int_{-1}^1 \left[\frac{\partial c_w^N}{\partial x}(t, x) \right]^2 w(x) dx \\ & + \frac{P\acute{e}}{2} [c_w^N(t, 1)]^2 \leq \sum_{k=0}^N f(c_w^N) c_w^N(t, x_k) w_k + \frac{P\acute{e}}{2} [c_w^N(t, -1)]^2. \end{aligned}$$

Integrating over the time interval $[0, t]$, we arrive at

$$\begin{aligned} & \sum_{k=0}^N [c_w^N(t, x_k)]^2 w_k + \frac{1}{2} \int_0^t \int_{-1}^1 \left[\frac{\partial c_w^N}{\partial x}(s, x) \right]^2 w(x) dx ds + P\acute{e} \int_0^t [c_w^N(s, 1)]^2 ds \\ & - P\acute{e} \int_0^t [c_w^N(s, -1)]^2 ds \leq 2 \int_0^t \sum_{k=0}^N f(c_w^N) c_w^N(s, x_k) w_k ds + \sum_{k=0}^N [c_w^N(0, x_k)]^2 w_k. \end{aligned}$$

Therefore, using the inequality $2xy \leq x^2 + y^2$ and the fact that the discrete and continuous norms are equivalent, we have

$$\begin{aligned} & \int_{-1}^1 [c_w^N(t, x)]^2 w(x) dx + \frac{1}{2} \int_0^t \int_{-1}^1 \left[\frac{\partial c_w^N}{\partial x}(s, x) \right]^2 w(x) dx ds \tag{6.3} \\ & + \underbrace{P\acute{e} \int_0^t [c_w^N(s, 1)]^2 ds - P\acute{e} \int_0^t [c_w^N(s, -1)]^2 ds}_{T_1} \\ & \leq \underbrace{\int_0^t \int_{-1}^1 (c_w^N(s, x))^2 w(x) dx ds}_{T_2} + \underbrace{\int_0^t \sum_{k=0}^N (f(c_w^N))^2 w_k ds}_{T_3} + \sum_{k=0}^N [c_w^N(0, x_k)]^2 w_k. \end{aligned}$$

Since the influx and outflux of the drug are identical, the term T_1 is zero unless some of it is absorbed, and some of it is wasted due to several factors such as blood flow and plasma. In this case, $T_1 > 0$ and we can ignore it.

Applying the mean value theorem for the term T_2 , we get

$$T_2 = \int_{-1}^1 (c_w^N(\eta, x))^2 w(x) dx \int_0^t ds, \quad \eta \in (0, t).$$

Since for every $\eta \in (0, t)$, we have $c_w^N(\eta, x) \leq B_0$, we may write

$$T_2 \leq T_f B_0^2 \int_{-1}^1 w(x) dx,$$

where $T_f = \max\{s : s \in (0, t)\}$.

Since $\beta_p > 0$ and $b_w^N(t, x_k)/b_{max} > 0$, we have

$$f(c_w^N(t, x_k)) \leq D_w^* B_0 [B_0 - b_w^N(t, x_k)/\beta_p].$$

As a result, we have

$$f(c_w^N(t, x_k)) \leq D_w^* B_0.$$

Imposing the above inequalities into T_3 and doing some manipulation, we obtain

$$T_3 \leq T_f \int_{-1}^1 D_w^* B_0^2 w(x) dx,$$

therefore, inequality (6.3) may be rewritten as

$$\begin{aligned} & \int_{-1}^1 [c_w^N(t, x)]^2 w(x) dx + \frac{1}{2} \int_0^t \int_{-1}^1 \left[\frac{\partial c_w^N}{\partial x}(s, x) \right]^2 w(x) dx ds \leq T_f \\ & \times \int_{-1}^1 (c_w^N(0, x))^2 w(x) dx + T_f \int_{-1}^1 (f(c_w^N(T_f, x)))^2 w(x) dx + \sum_{k=0}^N [c_w^N(0, x_k)]^2 w_k. \end{aligned}$$

This shows that the scheme (4.9) is stable. Similarly, repeating the above argument for Equation (3.2) we find that

$$\begin{aligned} & \int_{-1}^1 [c_c^N(t, x)]^2 w(x) dx + \frac{D}{2} \int_0^t \int_{-1}^1 \left[\frac{\partial c_c^N}{\partial x}(s, x) \right]^2 w(x) dx ds \leq T_f \\ & \times \int_{-1}^1 (c_c^N(\eta, 0))^2 w(x) dx + T_f \int_{-1}^1 (f(c_c^N(T_f, x)))^2 w(x) dx + \sum_{k=0}^N [c_c^N(0, x_k)]^2 w_k, \end{aligned}$$

which shows that the scheme (4.11) is stable.

Finally, to prove the convergence of the proposed scheme, we assume that the exact solution is smooth enough and define the interpolation operator I_N by

$$I_N c_J = \sum_{k=0}^N \tilde{c}_{J_k} p_k, \quad I_N c_J(x_i) = c_J(x_i), \quad k = 0, 1, \dots, N, \quad J = c \text{ and } w,$$

where \tilde{c}_{J_k} is called discrete polynomial coefficient of c_J and

$$\tilde{c}_{J_k} = \frac{1}{\alpha_k} \sum_{j=0}^N c_J(x_j) p_k(x_j) w_j, \quad k = 0, 1, \dots, N,$$

in which

$$\alpha_k = \sum_{j=0}^N p_k^2(x_j) w_j.$$

To get a convergence estimate, we set as usual

$$e(t, x_k) = \tilde{c}_J(t, x_k) - c_J^N(t, x_k).$$

Since for Chebyshev polynomial $\partial(I_N c_J)/\partial x \neq I_N \partial c_J/\partial x$, it follows that

$$\frac{\partial \tilde{c}_J}{\partial t}(t, x_k) - \frac{\partial^2 \tilde{c}_J}{\partial x^2}(t, x_k) = r_J(t, x_k), \quad r_J(t, x_k) = \frac{\partial^2(c_J - \tilde{c}_J)}{\partial x^2}.$$

Using the same analysis was discussed in the stability, yields

$$\begin{aligned} & \frac{1}{2} \frac{d}{dt} \sum_{k=0}^N [e(t, x_k)]^2 w_k + \frac{1}{4} \int_{-1}^1 \left[\frac{\partial e(t, x)}{\partial x} \right]^2 w(x) dx \\ & \leq \sum_{k=0}^N r_J(t, x_k) e(t, x_k) w_k \leq \sum_{k=0}^N [r_J(t, x_k)]^2 w_k + \sum_{k=0}^N [e(t, x_k)]^2 w_k. \end{aligned}$$

For any s on $[0, t]$, we set

$$\phi(s) = \sum_{k=0}^N [e(s, x_k)]^2 w_k, \quad g(s) = \sum_{k=0}^N [r_J(s, x_k)]^2 w_k.$$

Thanks to Gronwall lemma [3], it reads

$$\begin{aligned} & \sum_{k=0}^N [e(s, x_k)]^2 w_k + \underbrace{\frac{1}{2} \int_0^t \int_{-1}^1 \left[\frac{\partial e(z, x)}{\partial x} \right]^2 w(x) dx dz}_{T_2} \\ & \leq \exp(s) \int_0^t \sum_{k=0}^N [r_J(z, x_k)]^2 w_k dz. \end{aligned}$$

Since $T_2 \geq 0$, we get

$$\sum_{k=0}^N [\tilde{c}_J(s, x_k) - c_J^N(s, x_k)]^2 w_k \leq \exp(s) \int_0^t \sum_{k=0}^N [r_J(z, x_k)]^2 w_k dz.$$

According to

$$\sum_{k=0}^N [r_J(t, x_k)]^2 w_k = \sum_{k=0}^N [I_N r_J(t, x_k)]^2 w_k$$

and using equivalence of discrete and continuous norms for L_w^2 norm, we have

$$\begin{aligned} & \sum_{k=0}^N [I_N r_J(t, x_k)]^2 w_k \leq 2 \int_{-1}^1 [I_N r_J(t, x)]^2 w(x) dx \leq 4 \left(\int_{-1}^1 \right. \\ & \times \left. \left[\left(\frac{\partial^2 c_J}{\partial x^2} - I_N \frac{\partial^2 c_J}{\partial x^2} \right)(t, x) \right]^2 w(x) dx + \int_{-1}^1 \left[\frac{\partial^2}{\partial x^2} (c_J - I_N c_J)(t, x) \right]^2 w(x) dx \right). \end{aligned}$$

Again, utilizing equivalence of discrete and continuous norms, we get

$$\int_{-1}^1 \left[\left(\frac{\partial^2 c_J}{\partial x^2} - I_N \frac{\partial^2 c_J}{\partial x^2} \right)(t, x) \right]^2 w(x) dx \leq \sum_{k=0}^N \left[\left(\frac{\partial^2 c_J}{\partial x^2} - I_N \frac{\partial^2 c_J}{\partial x^2} \right)(t, x_k) \right]^2 w_k.$$

As $\frac{\partial^2 c_J}{\partial x^2}(t, x) = I_N \frac{\partial^2 c_J}{\partial x^2}(t, x)$ holds for collocation nodes, the right-hand side of the above equation is zero. Now, employing

$$\int_{-1}^1 \left[\frac{\partial^2}{\partial x^2} (c_J - I_N c_J)(t, x) \right]^2 w(x) dx \leq \|c_J - I_N c_J\|_{H_w^2(-1,1)}^2,$$

we find that

$$\sum_{k=0}^N [r_J(t, x_k)]^2 w_k \leq 4 \|c_J - I_N c_J\|_{H_w^2(-1,1)}^2.$$

Making use of the following estimation for evaluation of the interpolation error in all Sobolev norms (see, for example, (5.5.26) [3])

$$\|c_J - I_N c_J\|_{H_w^l(-1,1)} \leq C N^{2l-1-m} |c_J|_{H_w^{m;N}(-1,1)},$$

leads to

$$\sum_{k=0}^N [e(s, x_k)]^2 w_k \leq 4C^2 N^{6-2m} \exp(s) \left(\int_0^t |c_J(z)|_{H_w^{m;N}(-1,1)}^2 dz \right), \quad (6.4)$$

where C is a constant independent of N and c_J and $|\cdot|$ is a semi-norm defined as

$$|c_J(z)|_{H_w^{m;N}(-1,1)} = \left(\sum_{k=0}^N \|c_J^{(k)}\|_{L_w^2(-1,1)} \right)^{\frac{1}{2}}.$$

The inequality (6.4) proves that the presented scheme is convergent.

Table 1. Values of parameters.

Parameters	Symbol	Value	Unit
Determining the geometry [7]	α	$\frac{2}{3}$	—
Diffusion coefficient [13]	D_c	1.2×10^{-12}	$cm^2 s^{-1}$
Thickness of coating [13]	l_c	10^{-3}	cm
Dissolution rate [14]	β_c	1	$(mol\ cm^{-3})^{-\frac{2}{3}}$
Initial concentration in coating [2]	B	10^{-4}	$mol\ cm^{-3}$
Drug solubility [14]	S	$\frac{B}{10}$	—
Mass transfer coefficient [17]	P	10^{-6}	$cm\ s^{-1}$
Velocity [13]	ν	5.8×10^{-6}	$cm\ s^{-1}$
Diffusion coefficient in arterial wall [2]	D_w	2.5×10^{-6}	$cm^2\ s^{-1}$
Thickness of wall [11]	l_w	4.5×10^{-2}	cm
Association (forward) rate constant [18]	k_f	2×10^6	$(mol\ cm^{-3}\ s)^{-1}$
Dissolution (backward) rate constant [18]	k_r	5.2×10^{-3}	s^{-1}
Local density of binding sites [18]	b_{max}	3.66×10^{-7}	$mol\ cm^{-3}$
Conforming to experimental value [2]	λ_w	10^8	$cm\ s^{-1}$

7 Numerical results

To achieve the numerical results, we use uniform meshes in both intervals and divide the domain of the polymer coating and the arterial wall into N_0 and N_1 sub-interval, respectively. To demonstrate the applicability of the proposed scheme, let us consider $N_0 = 8$, $N_1 = 32$, $\Delta t = 10^{-4}$ and $\epsilon = 10^{-6}$, stopping criterion for Euler method, with data taken from Table 1. Figure 3 shows the behavior of the concentration of the dissolved drug, c_c , and the concentration of the undissolved drug, b_c , in the polymeric coating stent up to 10 hours. It

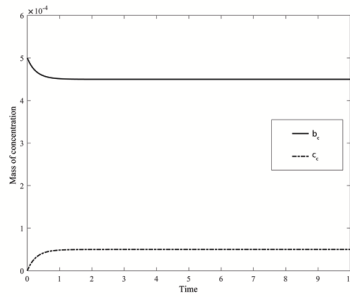


Figure 3. Concentration of the dissolved and undissolved drug in the polymeric coating stent for $T = 10$ and $\Delta t = 10^{-4}$.

demonstrates that the concentration of the dissolved drug (solid line) increases and the concentration of the undissolved drug (dash-dotted line) decreases as the loaded drug transferred to the dissolved drug during the process.

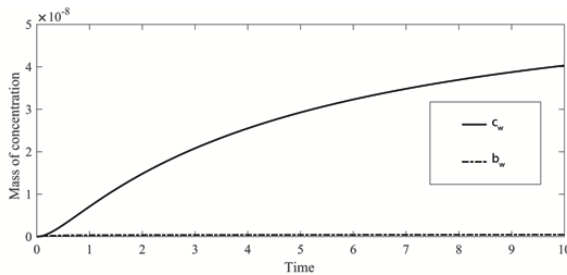


Figure 4. Concentration of the dissolved and binding drug in the arterial wall for $T = 1$ and $\Delta t = 10^{-4}$.

Figures 4 and 5 show the behavior of the concentration of the dissolved drug, c_w , and the concentration of the binding drug, b_w , in the arterial wall up to 1 and 10 hours, respectively. We observe that both concentrations are increasing as a function of time since the dissolved drug diffuses into the arterial wall whereas a number of it binds in the specified sites, which called the binding drug. Comparisons show a good agreement between the current study and available literature, while we have used much fewer mesh points.

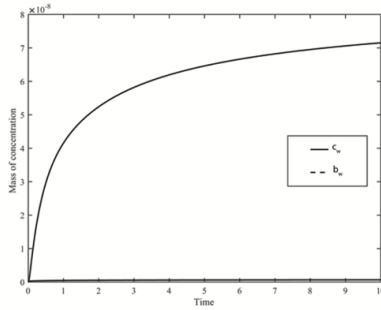


Figure 5. Concentration of the dissolved and binding drug in the arterial wall for $T = 10$ and $\Delta t = 10^{-4}$.

Tables 2 and 3 represent the maximum absolute error, MAE, given by

$$MAE = \max_{0 \leq j \leq N} |U^2(x_j) - U^1(x_j)|,$$

for the approximate solutions with the different value of mesh sizes. Here, U^2 and U^1 stand for the approximate solutions of the function with refinement mesh and coarse mesh, respectively. These tables report maximum absolute error for b_w and c_w with $(N_0, N_1) = (4, 16)$ and $(N_0, N_1) = (8, 32)$ in some specified collocation nodes, to be brief.

Table 2. Maximum absolute error for the dissolved drug (c_w) in the arterial wall with $N_0 = 4, N_1 = 16$ and $N_0 = 8, N_1 = 32$ in the modified Euler method.

k	MAE	k	MAE	k	MAE	k	MAE
1	0.00E+00	65	2.35E-14	129	5.93E-14	193	9.78E-14
2	0.00E+00	66	2.40E-14	130	5.99E-14	194	9.83E-14
3	8.33E-17	67	2.45E-14	131	6.05E-14	195	9.89E-14
4	1.60E-16	68	2.50E-14	132	6.11E-14	196	9.95E-14
5	2.78E-16	69	2.55E-14	133	6.17E-14	197	1.00E-13
6	4.51E-16	70	2.60E-14	134	6.23E-14	198	1.01E-13
⋮	⋮	⋮	⋮	⋮	⋮	⋮	⋮
60	2.10E-14	124	5.63E-14	188	9.47E-14	252	1.33E-13
61	2.15E-14	125	5.70E-14	189	9.53E-14	253	1.33E-13
62	2.20E-14	126	5.75E-14	190	9.60E-14	254	1.34E-13
63	2.25E-14	127	5.82E-14	191	9.65E-14	255	1.35E-13
64	2.29E-14	128	5.87E-14	192	9.71E-14	256	1.35E-13

8 Conclusions

The present work considers the Lagrange collocation method in combination with the modified Euler method to solve a comprehensive one-dimensional

Table 3. Maximum absolute error for the dissolved drug (b_w) in the arterial wall with $N_0 = 4, N_1 = 16$ and $N_0 = 8, N_1 = 32$ in the modified Euler method.

k	MAE	k	MAE	k	MAE	k	MAE
1	0.00E+00	65	4.45E-14	129	2.36E-13	193	6.01E-13
2	0.00E+00	66	4.63E-14	130	2.40E-13	194	6.09E-13
3	0.00E+00	67	4.81E-14	131	2.45E-13	195	6.16E-13
4	1.39E-17	68	4.99E-14	132	2.49E-13	196	6.23E-13
5	2.78E-17	69	5.17E-14	133	2.54E-13	197	6.30E-13
6	4.16E-17	70	5.36E-14	134	2.58E-13	198	6.38E-13
⋮	⋮	⋮	⋮	⋮	⋮	⋮	⋮
60	3.64E-14	124	2.15E-13	188	5.67E-13	252	1.09E-12
61	3.80E-14	125	2.19E-13	189	5.73E-13	253	1.10E-12
62	3.96E-14	126	2.23E-13	190	5.80E-13	254	1.11E-12
63	4.12E-14	127	2.27E-13	191	5.87E-13	255	1.12E-12
64	4.29E-14	128	2.32E-13	192	5.94E-13	256	1.13E-12

model of drug release from cardiovascular stents. In this paper, we have discretized the problem using nodal bases in the spatial dimension, using the characteristic Lagrange polynomial ψ_l of degree N in (4.2) and Gauss-Lobatto points as spatial discretization nodes. To reduce the effect of round-off errors resulting from the subtraction of nearly equal quantities, we have used (4.7) to calculate the nodal base derivative of the proposed spectral method. In the dimension of time, to make the method stable, we have used the backward Euler method. As well as. we proved the existence and uniqueness of the solution and performed consistency, stability, and convergence analyses of the proposed scheme. Obtaining numerical results, we observed that the proposed method, in addition to being stable and convergent, could give acceptable results with much fewer mesh points.

References

- [1] W.E. Boyce and R.C. DiPrima. *Elementary Differential Equations and Boundary Value Problems*. John Wiley & Sons, New York, United States, 7th edition, 2001. ISBN 0-471-31999-6.
- [2] F. Bozsak, J.M. Chomaz and A.I. Barakat. Modeling transport of drugs eluted from stents: physical phenomena driving drug distribution in the arterial wall. *Biomech. Model. Mechanobiol.*, **13**:327–347, 2014. <https://doi.org/10.1007/s10237-013-0546-4>.
- [3] C. Canuto, M. Hussaini, A. Quarteroni and T. Zang. *Spectral Methods: Fundamentals in Single Domains*. Springer-Verlag, Berlin, Heidelberg, 3rd edition, 2006. ISBN 978-3-540-30725-9.
- [4] C. D’Angelo, P. Zunino, A. Porpora, S. Morlacchi and F. Migliavacca. Model reduction strategies enable computational analysis of controlled drug release from cardiovascular stents. *SIAM J. Appl. Math.*, **71**(6):2312–2333, 2011. <https://doi.org/10.1137/10081695X>.

- [5] J.A. Ferreira, M. Grassi, E. Gudino and P. de Oliveria. A 3D model for mechanistic control of drug release. *SIAM J. Appl. Math.*, **74**(3):620–633, 2014. <https://doi.org/10.1137/130930674>.
- [6] J.A. Ferreira, J. Naghipoor, and P. de Oliveira. Analytical and numerical study of a coupled cardiovascular drug delivery model. *J. Comput. Appl. Math.*, **275**:433–446, 2015. <https://doi.org/10.1016/j.cam.2014.04.021>.
- [7] G. Frenning. Modelling drug release from inert matrix systems: From moving boundary to continuous-field descriptions. *Int. J. Pharm.*, **418**(1):88–99, 2011. <https://doi.org/10.1016/j.ijpharm.2010.11.030>.
- [8] E. Gudiño and A. Sequeira. 3D mathematical model for blood flow and non-Fickian mass transport by a coronary drug-eluting stent. *Appl. Math. Mod.*, **46**:161–180, 2017. <https://doi.org/10.1016/j.apm.2017.01.057>.
- [9] A.W. Hixson and J.H. Crowell. Dependence of reaction velocity upon surface and agitation. *Ind. Eng. Chem.*, **23**:923–931, 1931. <https://doi.org/10.1021/ie50260a018>.
- [10] M. Livingston and A. Tan. Coating techniques and release kinetics of drug-eluting stents. *J. Med. Devices.*, **10**(1):15–23, 2016. <https://doi.org/10.1115/1.4031718>.
- [11] X. Lu, J. Yang, J.B. Zhao, H. Gregersen and G.S. Kassab. Shear modulus of porcine coronary artery: contributions of media and adventitia. *Am. J. Physiol. Heart Circ. Physiol.*, **285**:H1966–H1975, 2003. <https://doi.org/10.1152/ajpheart.00357.2003>.
- [12] S. McGinty. *Stents and arterial flows*. PhD thesis, University of Strathclyde, Glasgow, UK, March 2010.
- [13] S. McGinty, S. McKee, R.M. Wadsworth and C. McCormick. Modeling arterial wall drug concentrations following the insertion of a drug-eluting stent. *SIAM J. Appl. Math.*, **73**(6):2004–2028, 2013. <https://doi.org/10.1137/12089065X>.
- [14] S. McGinty and G. Pontrelli. A general model of coupled drug release and tissue absorption for drug delivery devices. *J. Contr. Release.*, **217**:327–336, 2015. <https://doi.org/10.1016/j.jconrel.2015.09.025>.
- [15] A.A. Noyes and W.R. Whitney. The rate of solution of solid substances in their own solutions. *J. Am. Chem. Soc.*, **19**(12):930–934, 1897. <https://doi.org/10.1021/ja02086a003>.
- [16] H.K. Pathak. *An Introduction to Nonlinear Analysis and Fixed Point Theory*. Springer, Nature, Singapore, 2018. ISBN 978-981-10-8866-7.
- [17] G. Pontrelli and F. de Monte. Mass diffusion through two-layer porous media: an application to the drug-eluting stent. *Int. J. Heat Mass Transf.*, **50**(17-18):3658–3669, 2007. <https://doi.org/10.1016/j.ijheatmasstransfer.2006.11.003>.
- [18] A.R. Tzafiriri, A.D. Levin and E.R. Edelman. Diffusion-limited binding explains binary dose response for local arterial and tumour drug delivery. *Cell Prolif.*, **42**(3):348–363, 2009. <https://doi.org/10.1111/j.1365-2184.2009.00602.x>.
- [19] P. Zunino. Multidimensional pharmacokinetic models applied to the design of drug-eluting stents. *Int. J. Cardio. Eng.*, **4**(2):181–191, 2004. <https://doi.org/10.1023/B:CARE.0000031547.39178.cb>.
- [20] P. Zunino, C. D’Angelo, L. Petrini, C. Vergara, C. Capelli and F. Migliavacc. Numerical simulation of drug eluting coronary stents: mechanics, fluid dynamics and drug release. *Comput. Meth. Appl. Mech. Eng.*, **198**(45-46):3633–3644, 2009. <https://doi.org/10.1016/j.cma.2008.07.019>.